Available online at www.sciencedirect.com
SCIENCE DIRECT
Journal of Catalysis 240 (2006) 160–171
JOURNAL OF CATALYSIS
www.elsevier.com/locate/jcat

Highly dispersed platinum catalysts prepared by impregnation of texture-tailored carbon xerogels

Nathalie Job [a,*], Manuel Fernando Ribeiro Pereira [b], Stéphanie Lambert [a], Amandine Cabiac [c], Gérard Delahay [c], Jean-François Colomer [d], José Marien [e], José Luis Figueiredo [b], Jean-Paul Pirard [a]

[a] *Laboratoire de Génie Chimique, B6a, Université de Liège, B-4000 Liège, Belgium*
[b] *Laboratório de Catálise e Materiais, Departamento de Engenharia Química, Faculdade de Engenharia, Universidade do Porto, Rua Dr Roberto Frias, 4200-465 Porto, Portugal*
[c] *Laboratoire de Matériaux Catalytiques et Catalyse en Chimie Organique, UMR 5618-CNRS-ENSCM, Institut Charles Gerhardt FR 1878, 8 rue de l'Ecole Normale, F-34296 Montpellier cedex 5, France*
[d] *Laboratoire de Résonance Magnétique Nucléaire, Facultés Universitaires Notre-Dame de la Paix, rue de Bruxelles 61, B-5000 Namur, Belgium*
[e] *Laboratoire de Physicochimie des Surfaces, B6c, Université de Liège, B-4000 Liège, Belgium*

Received 22 December 2005; revised 17 March 2006; accepted 24 March 2006

Available online 24 April 2006

Abstract

Pt/C catalysts were prepared by impregnation of carbon xerogels with H_2PtCl_6 aqueous solutions. Three supports with various pore textures were used: two micro-mesoporous (maximum pore size = 10 and 40 nm, respectively) and one micro-macroporous (maximum pore size = 70 nm). After impregnation, drying and reduction, the metal particles were at most 1–1.5 nm in diameter. The Pt dispersion was close to 100% in the case of the xerogel with large mesopores. For the two other supports, a small fraction of Pt was trapped in blocked micropores. The specific catalytic activity obtained for benzene hydrogenation was 4–10 times higher than that obtained with active charcoal-supported catalysts prepared by a similar method. The high dispersion of Pt was attributed to the presence in the xerogel of large mesopore or macropore volumes, which facilitates impregnation, and a low amount of oxygenated surface groups.

Keywords: Carbon xerogel; Carbon support; Pt catalyst; Hydrogenation

1. Introduction

Carbon-supported catalysts are used in chemical industry for many applications. The most widely used supports are active charcoals, although carbon blacks or graphite are sometimes considered [1]. Compared with other catalyst supports, such as alumina and silica, carbon materials have many advantages: (i) they are stable in acid or basic media; (ii) they are resistant to high temperature; and (iii) the metal used as catalyst can be recovered easily after burning of the support. The catalysts are generally prepared by impregnation of a preexisting support with a solution of a metal salt. The various impregnation techniques differ from one another in terms of metal salt choice, solvent (polar or nonpolar), and postimpregnation treatments [1–3]. After impregnation, the catalyst is treated so as to obtain the active phase, (i.e., the metal in the reduced state) dispersed on the support. Metals are reduced under hydrogen at 200–500 °C, depending on the metal. The support properties (principally, surface composition and pore texture) are known to affect metal dispersion [1–6], although opinions about their relative importance vary.

Carbon materials issued from drying and pyrolysis of resorcinol–formaldehyde gels have not yet been widely studied. A few works are related to the use of carbon aerogels, porous carbon materials prepared by supercritical drying and

* Corresponding author. Fax: ++ 32 4 366 3545.
E-mail address: Nathalie.Job@ulg.ac.be (N. Job).

0021-9517/$ – see front matter
doi:10.1016/j.jcat.2006.03.016

pyrolysis of organic gels [7–11]. Examples concerning carbon xerogels are rare and very recent [12–14]. In these examples, xerogels were prepared from evaporative drying of the solvent after solvent exchange (water to acetone, generally), followed by pyrolysis; however, carbon xerogels with tailored texture can be prepared by simple evaporative drying, without pretreatment, of resorcinol–formaldehyde gels, provided that the correct synthesis conditions are chosen [15,16]. Indeed, micro-macroporous, micro-mesoporous, microporous, or nonporous carbon materials can be obtained by this method, the key variables being the pH and the dilution ratio of the precursors' solution. This kind of carbon material was recently used as a Pd and Pd–Ag catalyst support [17,18]. With regard to active charcoals, the advantages of carbon xerogels are their high purity and pore texture flexibility. Indeed, active charcoals are produced from natural sources like wood, nutshells, or fruit pits, and their pore texture is not easily controlled because it depends mainly on the structure of the pristine organic material [1]. Consequently, diffusional limitations often occur during catalytic processes. The pore texture of active charcoals can be modified to some extent by chemical and thermal treatments, but control of texture is very limited compared with that of carbon xerogels. The ash content of active charcoals can be very high (up to 15%), although choosing an adequate organic precursor can minimize the minerals loading. Finally, the pyrolysis temperature is usually high (from 800–1100 °C and even higher in some cases), and the carbon thus obtained is usually hydrophobic [4]. These properties are not ideal for impregnation with aqueous solutions, and active charcoals are often further partially oxidized to increase their mesopore or macropore volume and surface oxygen group content. The oxidation treatment can be performed in liquid phase, using HNO_3 or H_2O_2, or in gas phase, with oxygen. Another possibility is to use less or nonpolar solvents, such as acetone or cyclohexane; however, water is preferable for environmental and cost reasons. On the other hand, carbon xerogels are very hydrophilic after pyrolysis. Indeed, a micro-mesoporous or micro-macroporous carbon xerogel prepared by pyrolysis at 800 °C absorbs an amount of water corresponding to 95% of its pore volume within a few minutes, whatever the carbon texture. This type of support should then lead to a good metal dispersion. Moreover, it was recently shown that the presence of large amounts of mesopores or macropores allows minimizing or even suppressing diffusion limitations in the support [18].

The aim of the present work is to test carbon xerogels as supports for Pt/C catalysts. Carbon xerogel-supported catalysts were prepared by impregnating supports of various textures with hexachloroplatinatic acid aqueous solutions. After drying and reduction, the catalysts were characterized by X-ray diffraction, electron transmission microscopy, and CO chemisorption. The performance of these catalysts for benzene hydrogenation were compared with that of similar catalysts supported on commercial active charcoals and prepared by various methods. The results were analysed with regard to the carbon support texture and surface properties.

2. Experimental

2.1. Support and Pt/C catalyst synthesis

Pt/carbon xerogel catalysts were synthesized by impregnation of preexisting supports. Three carbon xerogels with various pore textures were selected: one micro-mesoporous support with small mesopores (10 nm), one micro-mesoporous support with large mesopores (40 nm), and one micro-macroporous support (70 nm). The three carbon xerogels were obtained from evaporative drying and pyrolysis of resorcinol–formaldehyde gels prepared following a method described in a previous study [15]. The resorcinol/formaldehyde molar ratio, R/F, was fixed at 0.5 and the dilution ratio, D (i.e., the solvent/(resorcinol + formaldehyde) molar ratio) was chosen equal to 5.7. Formaldehyde is available as an aqueous solution (37 wt% formaldehyde in water, stabilized by 10–15% methanol). Note that "solvent" in the dilution ratio takes into account the deionized water added, and the water and methanol contained in the formaldehyde solution. The pH of the three solutions was adjusted to 5.25, 5.60, and 6.25 with NaOH aqueous solutions. Gelation was performed at 85 °C, and the aging period at the same temperature was chosen to be 72 h. Note that this operation could be shortened to 24 h, as indicated by very recent results [19]. The obtained gels were then dried under vacuum without any pretreatment. The unsealed flasks were kept at 60 °C and the pressure was progressively reduced from 10^5 to 10^3 Pa. This step was performed over five days but can be shortened by using convective drying [19,20]. The samples were then heated to 150 °C at a pressure of 10^3 Pa for three days. After drying, pyrolysis was performed at 800 °C under flowing nitrogen and following the same temperature program as in previous studies [15–17]: (i) ramp at 1.7 °C min^{-1} to 150 °C and hold for 15 min; (ii) ramp at 5 °C min^{-1} to 400 °C and hold for 60 min; (iii) ramp at 5 °C min^{-1} to 800 °C and hold for 120 min; and (iv) cool slowly to room temperature. The carbon supports are denoted as follows: the letter X (for "xerogel") is followed by the initial pH of the precursor solution multiplied by 100. For example, X-525 is a carbon xerogel issued from drying and pyrolysis of a gel prepared at an initial pH of 5.25.

The carbon supports were crushed and sieved to prepare pellets of 1000–1250 μm in diameter. These pellets were impregnated with H_2PtCl_6 aqueous solutions. First, the incipient wetness method (i.e., impregnation with a quantity of solvent corresponding to the total pore volume of the support and containing the amount of metal to be dispersed on the carbons) was attempted. The advantage of this method is that all of the metal solubilized in the solvent is deposited on the support; the actual metal loading is known. Nevertheless, this method led to nonhomogeneous mixing; despite prolonged stirring, a large fraction of the support remained completely dry, while the impregnation solution was held in agglomerates of wet pellets. This is why the wet impregnation method (i.e., immersion of the support in an excess of impregnation solution) was finally chosen. Each crushed support was immersed in an aqueous solution of

Table 1
Composition of the impregnation solutions

Catalyst	V_v[a] ($cm^3\ g^{-1}$)	Pt_{th}[b] (wt%)	$m_{support}$[c] (g)	V_{HCP}[d] (cm^3)	V_{water}[e] (cm^3)
X-525-Pt	2.1	1	4	2.56	17.44
X-560-Pt	1.33	1	3	2.00	8.00
X-625-Pt	0.41	1	4	6.41	3.59

[a] V_v = total pore volume of the support.
[b] Pt_{th} = Pt nominal weight percentage.
[c] $m_{support}$ = mass of impregnated support.
[d] V_{HCP} = volume of $H_2PtCl_6{\cdot}6H_2O$ solution (concentration = 100 g/l).
[e] V_{water} = deionised water volume added.

hexachloroplatinic acid whose concentration was adjusted so that the theoretical metal loading was 1 wt%. The concentration of each solution was calculated as a function of the total pore volume of the support assuming that: (i) the concentration of the solution in excess after impregnation, eliminated by filtration, is identical to that of the initial solution; (ii) the metal can access the whole pore network of the support; (iii) the metal that entered the support remains trapped in the pore network after filtration and drying. The first hypothesis is valid only if the metal ions do not adsorb at the support surface, which is probably not the case; should adsorption and/or Pt(IV) reduction to Pt(II) occur, as observed in many works on the same subject [4], the actual metal loading would be greater than the nominal value. The smallest pores could also be inaccessible to the solution, which would induce the actual metal loading to be lower than the theoretical value. The actual metal amount deposited on the support is thus unknown and must be determined.

Three or four grams of the support, depending on its availability, were immersed in 10 cm^3 of the corresponding hexachloroplatinic aqueous solution. In the case of X-525, the amount of solution was 20 cm^3, because 10 cm^3 were not sufficient to obtain a homogeneous mix. An aqueous solution of $H_2PtCl_6{\cdot}6H_2O$ with a concentration equal to 100 g dm^{-3} was first prepared, then diluted to obtain three aqueous solutions adapted to the pore volume of the three carbon xerogels. The total pore volume of each support, V_v, necessary to the calculation of the solution concentration, is given in Table 1. It was determined from the combination of nitrogen adsorption and mercury porosimetry data (see Section 2.2). The composition of the solutions is also given in the same table.

After impregnation, the excess of solution was removed by filtration. The catalyst was dried under ambient air for 24 h, and then the remaining solvent was extracted under vacuum (10^3 Pa), at 60 °C for another 12 h. After drying, a fraction of each sample was reduced under hydrogen for 3 h at 350 °C. The hydrogen flow rate was fixed at 0.025 mmol s^{-1}, and the heating rate from ambient temperature to 350 °C was chosen to be equal to 350 °C h^{-1}. The reduced samples were used for characterization.

To denote the catalysts, the name of the support is followed by "Pt." For instance, X-525-Pt is the Pt/C catalyst prepared by impregnation of support X-525.

2.2. Support and Pt/C catalyst characterization

The pore texture of the support was characterized before and after impregnation, drying, and reduction treatments by the analysis of the nitrogen adsorption–desorption isotherms, performed at 77 K with a Sorptomatic Carlo Erba 1900 device. Before adsorption, the samples were outgassed at 10^{-3} Pa for 16 h. The analysis of the isotherms was performed according to the methodology proposed by Lecloux [21] and provided the BET specific surface area, S_{BET}, the micropore volume calculated by the Dubinin–Radushkevich equation, V_{DUB}, and the pore volume calculated from the adsorbed volume at saturation, V_p. For samples containing micropores and mesopores only and with an isotherm displaying a plateau at saturation, the nitrogen adsorption technique is sufficient for determining the total void volume; consequently, V_v and V_p are equal. Pore volume measurements by nitrogen adsorption are not sufficiently precise for samples containing macropores (pores of width >50 nm, corresponding to relative pressures $p/p_0 > 0.98$ following the Kelvin equation). In the case of micro-macroporous sample, mercury porosimetry was then used to measure the pore volume corresponding to pores >7.5 nm. After outgassing at 10^{-3} Pa for 2 h, mercury porosimetry measurements were performed between 0.01 and 0.1 MPa with a manual porosimeter, and between 0.1 and 200 MPa with a Carlo Erba Porosimeter 2000. The total pore volume, V_v, was then deduced from a combination of these two techniques [22],

$$V_v = V_{DUB} + V_{cum<7.5\ nm} + V_{Hg}, \quad (1)$$

where V_{DUB} takes into account pores of width <2 nm, V_{Hg} is the specific pore volume measured by mercury porosimetry, and $V_{cum<7.5\ nm}$ is the cumulative volume of pores of width 2–7.5 nm determined by the Broekhoff–de Boer theory [21]. In the case of micro-mesoporous carbons, the maximum pore diameter, $d_{p,max}$ (i.e., the pore diameter limit under which smaller pores represent 95% of the total pore volume) was deduced from pore size distributions provided by the Broekhoff–de-Boer method, assuming an open cylinder geometry. In the case of macroporous samples, the pore size distribution must be deduced from mercury porosimetry data. Because the macroporous samples undergo intrusion only during mercury pressure increase, the pore size distribution was calculated following Washburn's theory [23]. The bulk density of the materials, ρ_{bulk}, was measured by mercury pycnometry.

The oxygen surface groups of the supports before impregnation were characterized by temperature-programmed desorption (TPD). For each analysis, 200 mg of the support was heated at a rate of 5 °C min^{-1} under helium flow from ambient temperature up to 800 °C. The effluent composition was monitored continuously by sampling on-line to a Pfeiffer Omnistar quadruple mass spectrometer. The amounts of CO and CO_2 were obtained using a monohydrated calcium oxalate standard. The desorption profiles of CO and CO_2 are characteristic of specific surface groups [24,25].

The actual metal content of the catalysts after impregnation, drying, and reduction was measured by inductively coupled plasma–atomic emission spectrometry (ICP-AES), using an Iris

advantage Thermo Jarrel Ash device. The Pt solution was prepared as follows: first, 0.1 g of catalyst was digested by 20 mL of H_2SO_4 (95%) and 10 mL of HNO_3 (70%), then heated at 300 °C until the solution was clear (after about 16 h). After complete dissolution of the carbon support and evaporation, 3 mL of HNO_3 (70%) and 9 mL of HCl (38%) were added. The obtained solution was transferred into a 100-mL calibrated flask that was finally filled with deionized water.

Metal particles were examined by X-ray diffraction (XRD), transmission electron microscopy (TEM), and CO chemisorption. The XRD patterns were obtained with hand-pressed reduced samples mounted on a Siemens D5000 goniometer using the Cu-K_α line (Ni filter). Transmission electron micrographs were obtained with a Jeol 200 CX (200 kV) microscope. The reduced samples were crushed and dispersed in ethanol before being deposited on a copper grid. A volumetric static method was used for CO chemisorption [26,27]. Measurements were obtained on a Fisons Sorptomatic 1990 equipped with a turbomolecular vacuum pump that allows a high vacuum of 10^{-3} Pa. The nonreduced catalyst was first reduced in situ under hydrogen flow (0.0372 mmol s^{-1}); the samples were heated from 25 to 350 °C at a rate of 350 °C h^{-1} and kept at 350 °C for 3 h. After outgassing for 16 h at 340 °C, carbon monoxide adsorption was performed at 30 °C. Because both chemisorption (on the Pt surface atoms) and physisorption (on metallic sites and support surface) occur at the catalyst surface, chemisorption and physisorption effects must be separated. An initial CO adsorption isotherm was achieved to measure the total amount of adsorbed carbon monoxide (chemisorbed + physisorbed). The catalyst was then outgassed on the measurement unit at 30 °C for 2 h in a vacuum of 10^{-3} Pa, and a second CO adsorption isotherm was measured to evaluate the amount of physisorbed CO. The total chemisorbed amount of CO was deduced by subtracting the second isotherm from the first one and extrapolating the nearly horizontal difference curve to the uptake axis.

2.3. Catalytic tests: benzene hydrogenation

The catalysts were tested for the hydrogenation of benzene at 120, 130, 140, and 150 °C, at atmospheric pressure. The H_2/C_6H_6 molar ratio was fixed at 11. The C_6H_6 flow rate, controlled by a HPLC Gilson 305 pump, was 0.0455 mmol h^{-1}. All gas flows were adjusted by Bronkhorst mass flow controllers. A loops system located in the oven upstream from the reactor ensured the vaporization of benzene. The reactor, an Autoclave Engineers' BTRS, was enclosed in a convection oven with temperature controlled and programmed to within 0.1 °C using a thermocouple located inside the reactor envelope and a PID controller. Because the hydrogenation of benzene is highly exothermic ($-\Delta H_r = 213$ kJ mol^{-1} [28]), the temperature of the catalyst was also measured by a second thermocouple located just above the sample. The feed and the product streams were analysed on-line by a gas chromatograph equipped with a flame ionization detector.

For each test, 0.05 g of nonreduced catalyst, crushed and sieved again between 100 and 200 μm, was loaded into the reactor. Before the reaction, the catalyst was reduced under hydrogen; the reduction conditions were the same as those for the reduction of samples used for characterization (see Section 2.1). Each catalytic test started at 120 °C. This temperature level was maintained until a quasi-stationary state was observed (i.e., after about 2 h). Then the temperature was increased to 130, 140, and 150 °C, with the conversion measured for 30 min at each temperature step. In each case, a quasi-stationary state was observed.

The activity of the catalysts was calculated as the amount of benzene converted into cyclohexane per gram of Pt and per second. Because this reaction is structure-insensitive [29–31], the activity of the catalyst is directly linked to the amount of accessible metal atoms. Consequently, the catalytic activity is an indirect measurement of metal dispersion, defined as the amount of accessible metal atoms with regard to the total metal loading. The activation energy of the reaction catalysed by Pt was determined from measurements performed at various temperatures.

To compare the results obtained with data already published in literature for active charcoal supports, the reaction conditions chosen in this study were identical to those used by Aksoylu et al. [29–31], except for the catalyst mass (0.05 g instead of 0.25 g). Indeed, conversion values obtained with 0.25 g of Pt/carbon xerogel catalysts were systematically equal to 100% whatever the temperature. Therefore, the mass of catalyst was decreased down to the minimum amount allowed by the measurement device.

3. Results

3.1. Support and catalyst characterization

The textural characteristics of the three carbon xerogels, determined before impregnation, are reported in Table 2. The texture of the carbon xerogel varies greatly with the initial pH of the solution; the total pore volume, V_v, decreases from 2.1 to 0.41 $cm^3\ g^{-1}$ with a pH increase from 5.25 to 6.25. Fig. 1 shows the mesopore and macropore size distribution of the three supports. Sample X-525 is micro-macroporous with a maximum pore size close to 70 nm, sample X-560 is micro-mesoporous with large mesopores (maximum pore size = 40 nm), and sample X-625 is micro-mesoporous with small mesopores (maximum pore size = 10 nm).

Quantitative analysis results of the TPD profiles of the three carbon xerogels are given in Table 3. In general, in TPD experiments, CO_2 and CO desorption is observed, with CO_2 appearing at lower temperatures than CO [24,25]. This is due to the decomposition of the different oxygen-containing groups present on the carbon surface. The amounts of CO and CO_2 released from each support per gram of carbon, n_{CO} and n_{CO_2}, are very close and very low whatever the support; n_{CO} ranges from 374 to 530 μmol g_C^{-1}, and n_{CO_2} ranges from 119 to 192 μmol g_C^{-1}. The amount of oxygenated groups found in the carbon xerogels is comparable to those of nonoxidized activated carbons (cf., e.g., sample A1 in [25]). Much larger amounts can be incorporated after oxidation of the support in the case of both active charcoals and carbon xerogels [32]. In comparison, active

Table 2
Textural characteristics of the three supports and of the catalysts after impregnation, drying and reduction

Sample	S_{BET} ($m^2\,g^{-1}$)	V_{DUB} ($cm^3\,g^{-1}$)	V_p ($cm^3\,g^{-1}$)	V_{Hg} ($cm^3\,g^{-1}$)	V_v ($cm^3\,g^{-1}$)	$d_{p,max}$ (nm)	ρ_{bulk} ($g\,cm^{-3}$)	ε_p (–)	ρ_n ($g\,cm^{-3}$)	ε_n (–)
	±5	±0.01	±0.05	±0.05	±0.1	±1	±0.02	±0.02	±0.02	±0.02
Support before impregnation										
X-525	645	0.26	1.17	1.72	2.1	70[c]	0.40	0.73	1.40	0.38
X-560	615	0.25	1.29	1.06	1.33[b]	40[d]	0.56	0.61	1.42	0.36
X-625	600	0.25	0.41	–[a]	0.41[b]	10[d]	1.15	0.18	1.42	0.35
Catalyst										
X-525-Pt	545	0.22	1.14	1.73	2.0	70[c]	0.40	0.71	1.40	0.31[e]
X-560-Pt	545	0.24	1.30	1.05	1.30[b]	40[d]	0.57	0.60	1.42	0.35[e]
X-625-Pt	355	0.16	0.29	–[a]	0.29[b]	10[d]	1.19	0.15	1.42	0.23[e]

[a] – Not measurable (mesoporous sample—very small pores).
[b] ±0.05 $cm^3\,g^{-1}$ (micro-mesoporous sample: $V_v = V_p$).
[c] Obtained from Washburn's law (mercury porosimetry).
[d] Obtained from Broekhoff–de Boer's theory (nitrogen adsorption–desorption).
[e] Nodule void fraction remaining accessible after metal deposition.

Table 3
DTP results

Support	CO ($\mu mol\,g_C^{-1}$)	CO_2 ($\mu mol\,g_C^{-1}$)
X-525	530	119
X-560	447	177
X-575	374	192

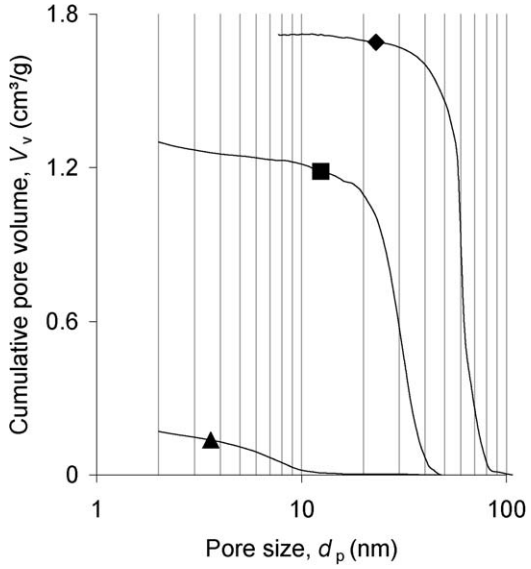

Fig. 1. Mesopore and macropore size distributions for the three carbon xerogel supports before impregnation: (◆) X-525, (■) X-560 and (▲) X-625.

charcoal oxidized with nitric acid or oxygen usually releases 6000–6500 $\mu mol_{CO}\,g_C^{-1}$ and 1000–1500 $\mu mol_{CO_2}\,g_C^{-1}$ [24,25]. Variations among the three carbon xerogel supports are very slight, and the surface composition can be considered quasi-constant.

After impregnation, drying, and reduction, the textural parameters of X-560-Pt do not change with regard to support X-560 (Table 2). For X-525-Pt, the specific surface area, S_{BET}, the micropore volume, V_{DUB}, and the total pore volume, V_v, decrease slightly ($V_v = 0.22\ cm^3\,g^{-1}$ and $S_{BET} = 545\ m^2\,g^{-1}$ compared with $V_v = 0.26\ cm^3\,g^{-1}$ and $S_{BET} = 645\ m^2\,g^{-1}$ before impregnation). In contrast, platinum deposition on X-625 strongly modifies S_{BET}, V_{DUB}, and V_v, in the resulting catalyst X-625-Pt; S_{BET} decreases from 600 to 355 $m^2\,g^{-1}$, V_{DUB} decreases to 0.16 from 0.25 $cm^3\,g^{-1}$ for the raw support, and V_v decreases from 0.41 to 0.29 $cm^3\,g^{-1}$. The pore volume corresponding to mesopores and macropores (i.e., $V_v - V_{DUB}$) remains almost constant, whatever the support. The maximum pore size, $d_{p,max}$, does not change. The shape of the hysteresis of adsorption–desorption isotherms (not shown) of the initial carbon supports remains identical, but the volume adsorbed at low relative pressure, p/p_0, which is related to microporosity, significantly decreases in X-625-Pt and X-525-Pt. These findings indicate that metal deposition affects microporosity only.

Table 4
Nominal and maximal platinum loading; ICP, XRD and CO chemisorption analysis results

Catalyst	Pt_{th}[a] (wt%)	Pt_{max}[b] (wt%)	ICP		XRD	CO
			Pt_{ICP}[c] (wt%)	$Pt_{\%}$[d] (%)	d_{XRD}[e] (nm)	$n_{s,m}$[f] ($mmol\,g_{Pt}^{-1}$)
X-525-Pt	1.0	2.4	1.9	77	<2	1.92
X-560-Pt	1.0	2.5	1.9	75	<2	3.14
X-625-Pt	1.0	6.0	4.5	75	<2	2.15

[a] Pt_{th}: nominal Pt loading.
[b] Pt_{max}: maximal Pt loading, solution in excess included.
[c] Pt_{ICP}: actual Pt loading measured by ICP-AES.
[d] $Pt_{\%}$: fraction of Pt deposited on the support with regard to the total amount contained in the impregnation solution.
[e] d_{XRD}: metal particle size obtained from X-ray diffraction (Scherrer's law).
[f] $n_{s,m}$: amount of CO needed to form a chemisorbed monolayer on the Pt surface atoms.

Table 4 displays the ICP analysis and CO chemisorption results. The metal loading measured by ICP, Pt_{ICP}, is systematically higher than the nominal value, Pt_{th} (1.9–4.5% compared with 1.0%). The higher the concentration of the hexachloroplatinic acid solution, the larger the difference between Pt_{th} and Pt_{ICP}. This result suggests the existence of interactions between the support and the hexachloroplatinate ions. Consequently, the concentration of the solution in excess should be lower than

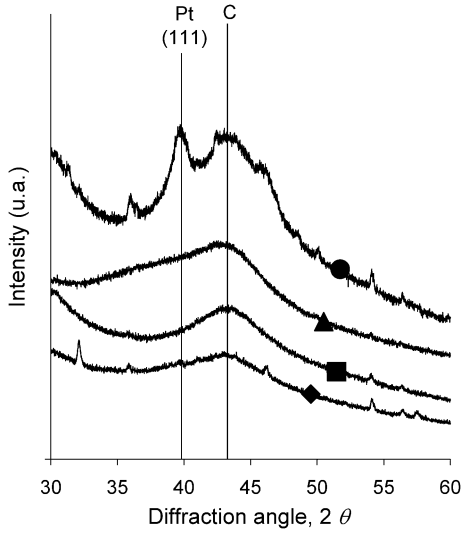

Fig. 2. X-ray diffraction performed on the catalysts after reduction. (◆) X-525-Pt; (■) X-560-Pt; (▲) X-625-Pt; (●) Pt/active charcoal (1 wt%, sample n°6 in [29]). The vertical lines mark the position of the most intense peak of Pt ($2\theta = 39.85°$) and graphite ($2\theta = 43.25°$). The curves were arbitrarily shifted upwards for clarity.

that of the initial solution. Indeed, the impregnation solution, which was bright yellow at the beginning, quickly faded during the support impregnation. The fraction of platinum actually deposited on the support, $Pt_{\%}$, can be calculated from the total amount of Pt contained in the impregnation solution, the mass of support used, and the actual metal content of the final catalyst. Whatever the carbon xerogel, $Pt_{\%}$ was identical (75–77%).

XRD results are presented in Fig. 2. For comparison, the diffractogram obtained with a Pt catalyst supported on a microporous active charcoal prepared in a comparable way is also shown. This latter sample (sample n°6) was synthesized in the context of a previous study [29]. The catalyst was prepared by incipient wetness impregnation of a commercial active charcoal Norit ROX with an H_2PtCl_6 aqueous solution. Before impregnation, the support was washed with HCl in aqueous phase and then oxidized with an O_2–N_2 mix (5–95%) in gas phase. The catalyst was thus reduced in hydrogen at 350 °C for 3 h. In Fig. 2, vertical lines indicate the position of the most intense Bragg lines of Pt and graphite. The (111) Bragg line of Pt is clearly visible in the case of the Pt/active charcoal sample. The mean Pt particle size, d_{XRD}, calculated from the peak broadening by Scherrer's law [26], is 5.0 nm, which is common for active charcoal-supported catalysts obtained by this impregnation method [29–31]. Other samples prepared by impregnation of commercial active charcoals by immersion in hexachloroplatinate acid aqueous solutions as described above led to similar metal particle sizes. Note that XRD is sensitive to the volume of particles; if the particle size distribution is not monodisperse, then the large particles have a greater influence on the diffraction signal, and Scherrer's law overestimates the mean particle size. Then d_{XRD} corresponds to the mean volume diameter (i.e., $d_v = \sum n_i d_i^4 / \sum n_i d_i^3$), where n_i is the number of particles with diameter equal to d_i. In the case of carbon xerogel-supported catalysts, the (111) Bragg line of Pt was barely detectable (X-625-Pt) or completely invisible (X-560-Pt and X-525-Pt). The detection limit of the Pt peak corresponded to particles with diameter close to 2 nm, indicating that the size of the metal particle dispersed on carbon xerogels was smaller than this value.

The amount of chemisorbed CO per Pt unit mass, $n_{s,m}$, ranged from 1.92 to 3.14 mmol g_{Pt}^{-1} for the xerogel series. These results again confirm the presence of Pt on the support and show that the accessible platinum surface was particularly high for X-560-Pt ($n_{s,m} = 3.14$ mmol g_{Pt}^{-1}, compared with 1.92 and 2.15 mmol g_{Pt}^{-1} for X-525-Pt and X-625-Pt, respectively). The analysis of the metal dispersion (i.e., the ratio between the number of metal atoms at the surface of the metal particles and the total number of metal atoms in those particles) is developed in Section 4.

Fig. 3 shows TEM micrographs of the three carbon xerogel-supported catalysts after metal reduction. For comparison, the Pt/active charcoal sample prepared in the previous study mentioned above [29] is also displayed. In the case of carbon xerogels, the metal particles were barely discernible from the support whatever the xerogel chosen (Figs. 3a, 3b and 3c); the particle size was close to the microscope detection limit. Due to astigmatism and image distortion, it was not possible to observe the samples at larger magnification. The diameter of the metal particles was <2 nm in each case and can be estimated as around 1.5 from TEM micrographs for X-625-Pt. The metal is even more difficult to distinguish in X-560-Pt and X-525-Pt; these catalysts probably contain particles <1 nm. These images confirm the XRD, CO chemisorption, and ICP analysis data indicating that the metal is present and very well dispersed on the support. For the active charcoal-supported catalyst shown in Fig. 2, the Pt particle diameter ranged from 3 to 5 nm (Fig. 3d).

3.2. Catalytic tests: benzene hydrogenation

Catalytic tests results are presented in Table 5. Benzene hydrogenation on Pt/carbon xerogel catalysts resulted in very high conversion ratios, even with very low catalyst amounts. The reaction conditions were identical to those used by Aksoylu et al. [29–31], except for the catalyst mass, which was decreased from 0.25 to 0.05 g so that the conversion was not >50%. Given the reactor dimensions (diameter = 6 mm), it was difficult to lower the catalyst mass below 0.05 g without risking insufficient contact between the catalyst and the reactants. The apparent reaction rate, r_a, was calculated from the conversion at every temperature for each catalyst.

For the carbon xerogel-supported catalysts, the apparent reaction rate ranged from 869 to 1842 μmol g_{Pt}^{-1} s^{-1} at 120 °C and from 1175 to 2513 μmol g_{Pt}^{-1} s^{-1} at 130 °C. At 140 °C, the conversion was >50% for all of the catalysts. At 150 °C, it was >70% for X-560-Pt and X-625-Pt; these results were not kept for further calculation. As a general comment, the apparent reaction rates per Pt mass unit were very high compared with those obtained in other studies with Pt/active charcoal catalysts prepared by impregnation of supports treated in various ways to increase the metal dispersion. As a comparison, Aksoylu et al. [29–31] mentioned apparent reaction rates ranging from 50

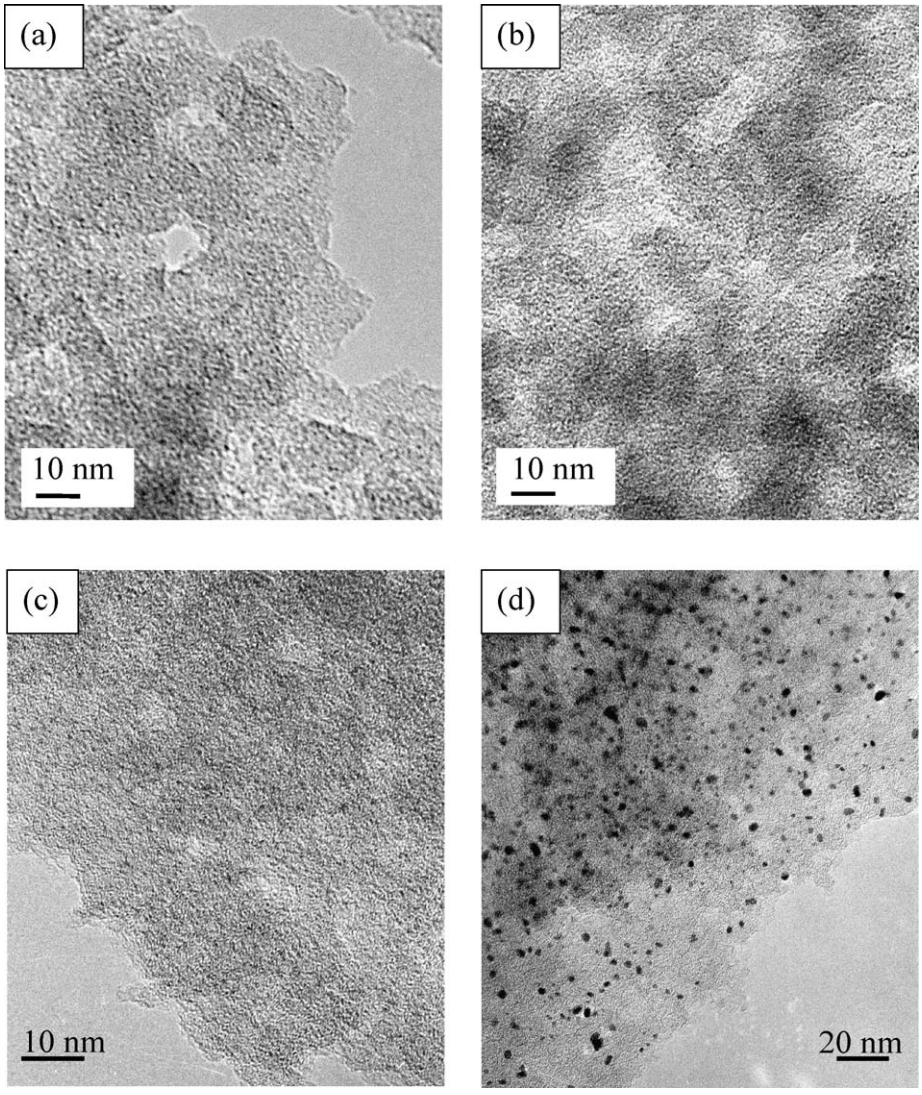

Fig. 3. Transmission electron microscopy: (a) X-525-Pt; (b) X-560-Pt; (c) X-625-Pt; (d) Pt/active charcoal (1 wt%, sample n°6 in [29]).

Table 5
Catalytic test results

Catalyst	r_a[a] (μmol g_{Pt}^{-1} s^{-1})			
	120 °C	130 °C	140 °C	150 °C
X-525-Pt	869	1203	1808[b]	2339[b]
X-560-Pt	1842	2513[b]	2840[b]	–[c]
X-625-Pt	1122	1175[b]	–[c]	–[c]

[a] r_a: apparent reaction rate for benzene hydrogenation per Pt mass unit.
[b] Conversion >50%.
[c] Conversion >70% (rejected results).

to 450 μmol g_{Pt}^{-1} s^{-1} for catalysts obtained by impregnation of active charcoals (preoxidized or not) with hexachloroplatinic acid aqueous solutions and tested under similar conditions. The best results (∼400 μmol g_{Pt}^{-1} s^{-1}) were obtained with preoxidized supports (e.g., sample n°6 in [29], whose XRD pattern and TEM micrographs are presented above). The activity of X-525-Pt and X-625-Pt was close to that of Pt/active charcoal catalysts prepared by organometallic chemical vapour deposition [31]. For active charcoals, this method leads to higher metal dispersion than impregnation but is also more complicated and expensive. The apparent reaction rate of sample X-560-Pt at 120 °C (1842 μmol g_{Pt}^{-1} s^{-1}) was about 10 times higher than that commonly observed with impregnated active charcoal and twice as high as that obtained with active charcoal-supported catalysts prepared by organometallic chemical vapour deposition.

The reaction rate observed is an apparent reaction rate. It equals the intrinsic reaction rate when no diffusional limitation occurs and when the reactor is differential only. As a first approximation, the reactor can be considered differential when the kinetic measurements are performed below 120 °C (conversion <40%). But this hypothesis is no longer acceptable for higher temperature ($T = 130$ °C; conversion of 40–60%). Results are processed below considering a differential reactor at 120 °C and an integral reactor when measurements obtained at 130, 140, and 150 °C are used. The existence of diffusional limitations can be highlighted by evaluating the Weisz modulus, Φ [33],

$$\Phi = \frac{r_a \rho_{bulk} L^2}{D_e C_s}, \tag{2}$$

where r_a is the observed reaction rate (mmol kg_{cat}^{-1} s^{-1}), ρ_{bulk} is the bulk density of the catalyst (kg_{cat} m^{-3}), L is the ratio between the volume and the external surface of the porous pellet (m), D_e is the effective diffusion coefficient of benzene (m^2 s^{-1}), and C_s is the benzene concentration at the pellet surface (mmol m^{-3}). In the case of spherical pellets, $L = d/6$, where d is the pellet diameter. The Weisz modulus compares the observed reaction rate to the diffusion rate. When $\Phi \ll 1$, the diffusion phenomenon has no significant effect, and r_a is equal to the intrinsic reaction rate. When $\Phi \gg 1$, diffusional limitations modify the apparent kinetics, and r_a can be very different from the intrinsic reaction rate. The effective diffusion coefficient, D_e, can be developed as a combination of the molecular diffusion, D_m, and the Knudsen diffusivity (Bosanquet formula [33]),

$$D_e = \left(\frac{(1/D_m) + (2/(97 \times 10^{-3} d_p \sqrt{T/M}))}{\varepsilon^2} \right)^{-1}, \quad (3)$$

where ε is the accessible void fraction of the catalyst pellet, d_p is the pore size (m), M is the molar weight of benzene (78.11×10^{-6} kg mmol^{-1}), T is the temperature expressed in K, and D_m is the molecular diffusivity of benzene in the fluid phase (m^2 s^{-1}), considered equal to that of benzene in hydrogen. D_m can be calculated as a function of the temperature by the Chapman–Enskog equation [33]: between 120 and 150 °C, D_m ranges from 1.61×10^{-4} to 1.39×10^{-4} m^2 s^{-1}. Because carbon xerogels are composed of interconnected microporous nodules separated by mesopores or macropores, the catalyst pellet can be considered to be composed of two separate levels [18,34,35], a first level corresponding to the pellet itself and a second level corresponding to the nodules. Each level is characterized by its own pore size, bulk density, void fraction, and characteristic dimension L [18,34,35]. The Weisz modulus can be calculated for both the pellet and nodule levels to determine the importance of diffusional limitations at any level.

At the pellet level, ρ_{bulk} is given in Table 2 (X-525-Pt, 400 kg m^{-3}; X-560-Pt, 570 kg m^{-3}; X-625-Pt, 1190 kg m^{-3}). To consider the most unfavourable case (i.e., the conditions leading to the slowest diffusion rate), d_p was chosen equal to the smallest mesopore or macropore size, that is, the pore width limit above which larger pores represent 95% of the total pore volume. Fig. 1 gives the values for d_p (X-525-Pt, $d_p = 40$ nm; X-560-Pt, $d_p = 20$ nm; X-625-Pt, $d_p = 4$ nm). At the pellet level, only diffusion from the pellet surface to the nodule surface was taken into account. Thus, the void fraction considered was that of the pellets, micropores excluded, ε_p. This parameter was calculated as

$$\varepsilon_p = \frac{V_v - V_{DUB}}{(1/\rho_{bulk})}. \quad (4)$$

Here ε_p ranged from 0.71 (X-525-Pt) to 0.15 (X-625-Pt) (Table 2). Considering that external diffusional limitations were negligible for the conditions chosen, C_s was equal to the benzene concentration in the gas flow. Again, the most unfavourable conditions were obtained when the reactant concentration was minimal, that is, when C_s was equal to the outlet concentration, which ranges from 900 to 1600 mmol m^{-3}. This method led to Weisz modulus values at the pellet level ranging from 10^{-2} to 10^{-5}, depending on the reaction conditions and on the catalyst. These findings indicate that no diffusional limitations occurred at the pellet level.

At the nodule level, TEM micrographs show that L varied from 10 to 100 nm. The bulk density, $\rho_{bulk,}$ was replaced by the bulk density of the nodules, ρ_n, which can be calculated as:

$$\rho_n = \left(\frac{1}{\rho_s} + V_{DUB} \right)^{-1}, \quad (5)$$

where ρ_s is the skeletal density of the carbon support and V_{DUB} is the micropore volume of the support before impregnation: indeed, micropores blocking may lead to decreasing micropore volume detected by nitrogen adsorption, but this phenomenon does not significantly alter the nodule density. In previous studies [15,16], ρ_s was measured by helium pycnometry and found to be constant and equal to about 2200 kg m^{-3}. Because V_{DUB} was quasi-constant in each support before impregnation, whatever the carbon xerogel used, the nodule bulk density, ρ_n, was constant as well (Table 2; $\rho_n \sim 1400$–1420 kg m^{-3}). The void fraction considered was that remaining accessible to gases after metal deposition, that is,

$$\varepsilon_n = \frac{V_{DUB}}{(1/\rho_{bulk}) - (V_v - V_{DUB})}, \quad (6)$$

where V_{DUB} and V_v are the micropore volume and the total pore volume of the final catalyst, respectively. Due to micropore blocking (and V_{DUB} variation), ε_n varied among the catalysts, ranging from 0.31 to 0.23 (Table 2). Because no diffusional limitations occurred at the upper level, the reactant concentration remained equal to that in the gas flow at the reactor outlet (900–1600 mmol m^{-3}). Calculations show that the Weisz modulus at the nodule level was always $<10^{-8}$. Thus the catalysts were operating in a chemical regime; the effect of the reactants diffusion on the observed kinetics was negligible.

Considering an integral isotherm reactor working in stationary state and a first-order reaction, the relationship between the conversion (f) and the apparent activation energy of the reaction (E_a) can be written as [33]

$$\ln\left(\ln \frac{1}{1-f} \right) = \ln C - \frac{E_a}{RT}, \quad (7)$$

where C is a constant, R is the perfect gas constant, and T is the temperature. The apparent activation energy for benzene hydrogenation on Pt was calculated from experimental data obtained at 120, 130, 140, and 150 °C. E_a was found to range from 57 to 64 kJ mol^{-1}, in agreement with values reported in the literature (30–70 kJ mol^{-1} [36]).

4. Discussion

According to several earlier studies carried out with Pt/active charcoal catalysts, metal dispersion essentially depends on two parameters: support pore texture and surface composition [1,4]. The surface composition determines the interactions between the support and the species to be deposited, as well as the

interactions between the solvent and the support. The presence in the carbon support of oxygenated surface groups, such as carboxylic acid, phenol, lactone, and carboxylic anhydride, enhances dispersion after the impregnation step [4–6]. The increased dispersion is attributed to interactions between the metal ion and the carbon surface via adsorption sites and, when a polar solvent (e.g., water) is used, to increased wettability of the carbon support, which facilitates penetration of the solution into the pore network. In the same way, the pore texture configuration plays an important role during impregnation [1,4]. On the one hand, the larger the pores, the more accessible the internal surface of the support; on the other hand, the larger the total accessible surface, the lower the interactions between the metal particles, and these particles then tend to remain small after reduction.

The influence of the carbon surface composition is also very important during the reduction treatment, which is performed between 200 and 500 °C depending on the metal. Indeed, the sintering of metal particles depends strongly on their local interactions with the support, and these interactions are defined by the chemical functions present at the carbon surface. The oxygenated groups seem to have a negative effect on the platinum dispersion after reduction [4]. This effect is attributed to a delocalisation modification of the aromatic cycles π-electrons of the carbon, which are responsible for anchoring of the reduced metal particles. This indicates that the same property of the carbon material may have diametrically opposite effects on the metal dispersion during successive treatments, and that a good metal dispersion generally results from a compromise; the oxygenated groups, which are necessary for an optimal impregnation by aqueous solutions, should be eliminated during the reduction step to avoid metal sintering. Rodríguez-Reinoso [4] concluded that the Pt dispersion on carbon supports is better when the support contains only oxygenated groups that are eliminated at relatively low temperatures.

The pore texture of active charcoals is usually much less homogeneous than that of carbon xerogels. Active charcoals can be considered to be composed of entirely microporous zones separated from each other by mesopores and/or macropores. The size distribution of these mesopores and macropores is generally very wide (from a few nanometers to several micrometers), but the corresponding total pore volume is usually rather low ($<0.5\ \mathrm{cm^3\,g^{-1}}$). This configuration is not optimal for impregnation, and the active charcoals are often partially oxidized with HNO_3 or H_2O_2 in liquid phase or with O_2 or N_2O in gas phase to increase the hydrophilicity of the support, so that the impregnation solution enters the micropores. In contrast, carbon xerogels contain high mesopore or macropore volume and have a very homogeneous pore texture. Thus, the pore texture of carbon xerogels is much more favourable to liquid absorption; the presence of oxygenated groups could be less crucial than in the case of active charcoals. The oxygenated groups content of carbon xerogels, measured by TPD, is about 10 times lower than that of oxidized active charcoals. Nevertheless, hexachloroplatinic acid aqueous solutions easily enter the pore network of carbon xerogels; within a few minutes, this kind of support absorbs an amount of water corresponding to 95% of its pore volume.

According to the conclusions of Rodríguez-Reinoso [4], this situation is optimal for obtaining high Pt dispersion values. Indeed, the amount of oxygenated groups that resist reduction at 350 °C (i.e., phenol, ether, carbonyl, quinone, and lactone) is very low. The presence of both large mesopore or macropore volume and low surface oxygenated group content could explain the drastic decrease in the metal particle size with regard to the results obtained by impregnation of active charcoals, preoxidized or not, with H_2PtCl_6 aqueous solutions. Also note that the actual Pt content in each catalyst is higher than the nominal value (1.9–4.5 wt% compared with 1 wt%), suggesting that interactions exist between the support and the metal ions during the impregnation step.

The platinum dispersion, D_{Pt} (i.e., the ratio between the number of surface Pt atoms and the total amount of Pt atoms) is given by [27]

$$D_{\mathrm{Pt}} = n_{\mathrm{s,m}} M_{\mathrm{Pt}} X_{\mathrm{Pt-CO}} \times 10^{-3}, \tag{8}$$

where $n_{\mathrm{s,m}}$ is the amount of CO needed to form a chemisorbed monolayer on surface Pt atoms ($\mathrm{mmol\,g_{Pt}^{-1}}$) and M_{Pt} is the atomic weight of Pt ($195.09\ \mathrm{g\,mol^{-1}}$). $X_{\mathrm{Pt-CO}}$ represents the chemisorption mean stoichiometry, that is, the mean number of Pt atoms on which one CO molecule is adsorbed. The knowledge of the adsorption stoichiometry is necessary for the analysis of CO chemisorption data. Indeed, CO can form linear or bridged bonds with surface Pt atoms. Other types of bonds exist (e.g., a "crown bond" between three Pt atoms and one CO molecule [27]), but these configurations are much less common. The ratio of linear to bridged bonds depends on the size and structure of the Pt particles. In particular, the presence of edges, steps, and crystallographic imperfections at the metal particle surface has a strong influence on the bond type [27].

In most studies performed on Pt/C catalysts with dispersion ranging between 15 and 25%, $X_{\mathrm{Pt-CO}}$ is considered equal to unity [37]; in other words, all CO–Pt bonds are considered linear. However, Rodríguez-Reinoso et al. [38] showed that in the case of high dispersion values ($25\% < D_{\mathrm{Pt}} < 50\%$), $X_{\mathrm{Pt-CO}}$ increases; bridged bonds are formed to the detriment of linear bonds. In this study, CO chemisorption and H_2 chemisorption results were compared, considering that the Pt–H adsorption stoichiometry remains equal to unity whatever the metal dispersion. At low dispersion value (<25%), the amount of adsorbed CO was equal to that of adsorbed hydrogen, and the CO adsorption stoichiometry was $X_{\mathrm{Pt-CO}} = 1$. But as the dispersion increased, the relationship between adsorbed CO and adsorbed hydrogen changed. The correlation straight line between the amounts of adsorbed CO and adsorbed hydrogen showed that when the Pt dispersion exceeded 25%, $X_{\mathrm{Pt-CO}} = 1.61$, indicating the presence of bridged bonds between Pt and CO. The proposed explanation for this finding is that the formation of bridged bonds is favoured when the Pt atoms are located at edges of the Pt crystal or at a crystallographic defect. The amount of such adsorption sites increases when the size of the metal particles decreases.

Table 6
Dispersion and equivalent metal particle size[a]

Catalyst	$X_{Pt–CO} = 1$		$X_{Pt–CO} = 1.61$		$X_{Pt–CO} = 2$	
	D_{Pt} (%)	d_{CO} (nm)	D_{Pt} (%)	d_{CO} (nm)	D_{Pt} (%)	d_{CO} (nm)
X-525-Pt	34	3.3	54	2.1	67	1.7
X-560-Pt	61	1.8	99	1.1[b]	122[c]	–[d]
X-625-Pt	41	2.8	66	1.7	82	1.4

[a] $X_{Pt–CO}$ = mean CO–Pt chemisorption stoichiometry; D_{Pt} = platinum dispersion; d_{CO} = equivalent diameter of the metal particles obtained by CO chemisorption.
[b] Maximum value: all the Pt atoms are accessible.
[c] Absurd value (>100%).
[d] Not calculated, the dispersion value obtained being absurd.

Note that the metal particles studied by Rodríguez-Reinoso et al. in the study summarized above [38] were never smaller than 2 nm in diameter. Consequently, the stoichiometry to be considered for the analysis of the metal dispersion of Pt/carbon xerogel catalysts could deviate from $X_{Pt–CO} = 1.61$. The CO chemisorption data were thus analysed using three values of the adsorption stoichiometry: $X_{Pt–CO} = 1$ (i.e., CO adsorbs on Pt via linear bonds only); $X_{Pt–CO} = 1.61$ (i.e., the bridged and linear bonds coexist, and the ratio between the two bond types is the same as that observed when D_{Pt} ranges from 25 to 50% by Rodríguez-Reinoso et al. [38]); and $X_{Pt–CO} = 2$ (i.e., bridged bonds exist only between Pt and chemisorbed CO). The mean equivalent particle diameter, d_{CO} (i.e., the particle diameter leading to a metal surface equivalent to that detected by chemisorption) can be calculated by [27]

$$d_{CO} = \frac{6(v_m/a_m)}{D_{Pt}}, \tag{9}$$

where v_m is the mean volume occupied by a metal atom in the bulk of a metal particle (for Pt, $v_m = 0.0151$ nm^3) and a_m is the mean surface area occupied by a surface metal atom (for Pt, $a_m = 0.0807$ nm^2) [27]. The values of D_{Pt} and d_{CO} obtained with the three chemisorption stoichiometries considered are displayed in Table 6.

Results obtained with $X_{Pt–CO} = 1$ led to mean particle sizes d_{CO} clearly larger than those observed by TEM and XRD. For X-525-Pt and X-625-Pt, $d_{CO} = 3.3$ and 2.8 nm, respectively. However, 3 nm particles should be detected by XRD, and TEM images showed that the metal particles were 1–1.5 nm maximum. For X-560-Pt, the results were in good agreement with XRD results ($d_{CO} = 1.8$ nm, not easily detectable by XRD), but the particle size observed by TEM was <1.5 nm. These results indicate either that the metal was partly inaccessible or the chemisorption stoichiometry $X_{Pt–CO}$ was underestimated. For X-525-Pt and X-625-Pt, a fraction of the metal possibly was entrapped in micropores blocked by other metal particles. Indeed, nitrogen adsorption–desorption measurements showed that the specific surface area, S_{BET}, decreased in both samples after impregnation. This phenomenon was not observed with X-560-Pt; all of the Pt particles should be accessible in this catalyst.

Considering $X_{Pt–CO} = 2$ leads to an absurd result for X-560-Pt ($D_{Pt} > 100\%$); in this case, the only explanation is that the adsorption stoichiometry was not chosen appropriately. CO chemisorption results obtained with the two other catalysts are in good agreement with the metal particle size derived from other techniques if all of the metal is assumed to be accessible. This hypothesis is probably valid for X-560-Pt; the specific surface area and total pore volume of the support did not decrease after impregnation. However, assuming that all of the metal is accessible in X-525-Pt and X-625-Pt is doubtful, because the total pore volume decreased from 0.26 to 0.22 cm^3 g^{-1} and from 0.25 to 0.16 cm^3 g^{-1}, respectively.

Finally, the intermediate stoichiometry value ($X_{Pt–CO} = 1.61$) led to plausible results for the three carbon xerogel-supported catalysts. Note that the metal particle size calculated for X-560-Pt using $X_{Pt–CO} = 1.61$ as adsorption stoichiometry parameter (i.e., $d_{CO} = 1.1$ nm) was a maximum value. Indeed, because all of the metal atoms are accessible ($D_{Pt} = 99\%$), it is not possible to calculate the mean metal particle diameter from Eq. (9): the number of accessible atoms detected by CO chemisorption is the same whatever the particle size when the metal particles are <1.1 nm. Given the size of a Pt atom (0.276 nm diameter), X-560-Pt probably should be considered to comprise aggregates composed of a few metal atoms (2–10 units) deposited on the carbon support. The Pt atoms cannot be isolated from one another; otherwise, it would not be possible to form bridged bonds between Pt and CO, and the chemisorption stoichiometry to be considered would be $X_{Pt–CO} = 1$.

These results illustrate the difficulties encountered when the accessible metal surface is analysed by CO chemisorption. Because the two extreme values of chemisorption stoichiometry ($X_{Pt–CO} = 1$ or 2) led to particle sizes inconsistent with the TEM and XRD observations or to absurd results, the intermediary value of $X_{Pt–CO}$ seems to be the best choice. Nevertheless, it is also possible that the stoichiometry to consider is not the same for all catalysts.

The hydrogenation of benzene is a structure-insensitive reaction [29–31]. In other words, in principle, the reaction rate is directly proportional to the accessible Pt surface (i.e., to the metal dispersion). Consequently, the reaction rate, expressed in μmol of benzene transformed into hexane per second and per catalyst unit mass (support included), is proportional to the amount of CO chemisorbed per catalyst unit mass provided that the chemisorption stoichiometry does not change with the metal dispersion. Fig. 4a shows that for the three carbon xerogel-supported catalysts with varying dispersion values, the relationship between the reaction rate and the amount of chemisorbed CO is linear. This suggests that the CO chemisorption stoichiometry can be considered identical in the three samples. Because the intermediary stoichiometry ($X_{Pt–CO} = 1.61$) seems the most likely for X-560-Pt, this value was finally selected for the three catalysts. The results are thus in agreement with those of Rodríguez-Reinoso et al. [38]. Fig. 4b shows that the relationship between the catalytic activity at 120 °C, expressed in μmol of benzene transformed into hexane per unit mass of Pt and per second, and the Pt dispersion, D_{Pt}, is almost linear. The straight line passes through the axis origin. The gap between the experimental data and the linear regression can be due to slight differences between the actual adsorption stoichiometries of the three catalysts. More probably, the fact that the reactor is

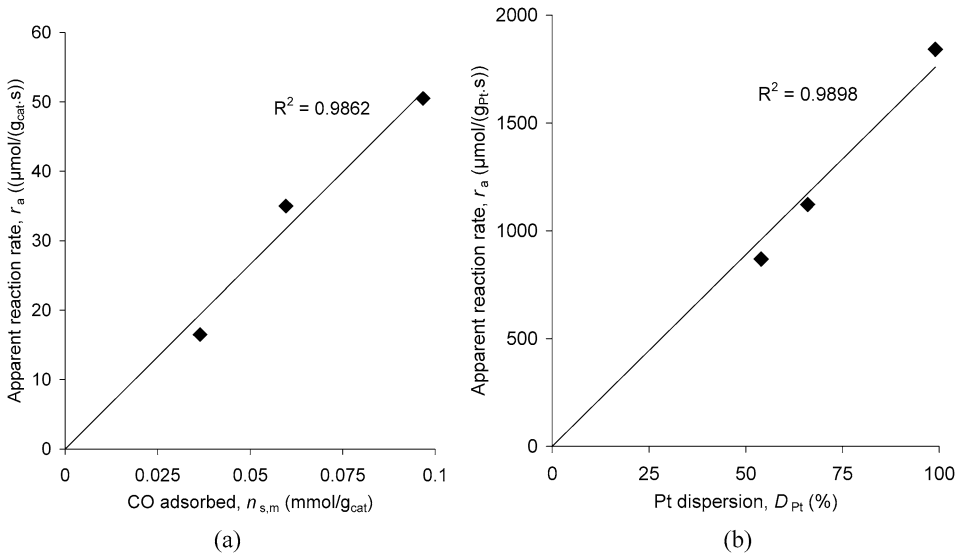

Fig. 4. (a) Relationship between the apparent reaction rate, r_a, and the amount of chemisorbed CO, $n_{s,m}$, both expressed by unit mass of catalyst; (b) relationship between the apparent reaction rate, r_a, expressed by unit mass of metal, and the platinum dispersion, D_{Pt}, considering $X_{Pt–CO} = 1.61$. N.B.: The apparent reaction rate values, r_a, are those obtained at 120 °C, i.e., when the reactor can reasonably be considered as differential.

not differential induces errors in the catalyst activity measurements.

5. Conclusion

Highly dispersed Pt/C catalysts were obtained by simple immersion of carbon xerogels in hexachloroplatinic acid solutions, followed by drying and reduction. Three supports with various maximal pore sizes (10, 40, and 70 nm) were used as supports. After the removal of excess solvent by filtration, followed by drying and reduction, the metal particles were very small; the TEM and XRD detection limits were reached, and the metal particle size was probably at most 1.5 nm in each xerogel-supported catalyst. Here, the term "metal particle" likely is not appropriate for such small objects; platinum is dispersed on the carbon supports as aggregates composed of a few atoms (probably up to a dozen).

The accessible metal surface depends on the xerogel texture. The metal dispersion was found to be maximal for the support containing large mesopores (40 nm); indeed, almost all of the Pt atoms were accessible, and the benzene hydrogenation reaction rate per Pt unit mass was maximal. For the two other supports, blocking of the microporosity was detected. Therefore, it can be suggested that some particles were probably accessible only from one side or were completely enclosed in blocked micropores. The metal was not fully accessible because of its insertion in micropores. For the support containing small mesopores, the decreased dispersion value (from 99 to 66%) was also probably due to a slight increase in metal cluster size (as shown by TEM and XRD). The benzene hydrogenation rate was 4 to 10 times higher than that obtained with Pt/active charcoal catalysts prepared similarly, depending on the metal dispersion.

The very high dispersion of Pt can be attributed to two parameters: the texture and surface composition of the carbon xerogel. In active charcoals, oxygenated groups are usually needed to render the support hydrophilic; otherwise, the impregnation solution has difficulty entering the micropores. This is why this kind of support is often pretreated with nitric acid, hydrogen peroxide, oxygen, or other oxidants. Nevertheless, these oxygenated groups tend to favour metal sintering when they resist the reduction treatment. Although the carbon xerogels contain very low amounts of oxygenated groups, the presence of large mesopore or macropore volume facilitates entry of the impregnation solution into the pore network. The amount of oxygenated groups that resist reduction at 350 °C (i.e., lactone, quinone, phenol, carbonyl, and carboxylic anhydride) is about 10 times lower in carbon xerogels than in preoxidized active charcoals. Consequently, when dispersed on carbon xerogel, the metal remains extremely well dispersed, and the catalytic performance is better than that of active charcoal-supported catalysts prepared by impregnation. Moreover, the preparation method is very simple and can be used at a larger scale.

These results obtained with carbon xerogels as metal supports are very encouraging, demonstrating the usefulness of this kind of support for heterogeneous catalysis. Research perspectives are numerous. In particular, the influence of the surface composition should be studied to gain more insight into the mechanisms leading to very well-dispersed catalysts supported on carbon materials.

Acknowledgments

The authors thank the Belgian Fonds National de la Recherche Scientifique (FNRS), the Région Wallonne Direction Générale des Technologies, de la Recherche et de l'Energie, the Ministère de la Communauté française, Direction de la Recherche scientifique and the Fonds de Bay for financial support. Jean-François Colomer thanks the FNRS (Belgium) for a research fellowship. The Belgian authors also acknowledge the involvement of their laboratory in the Network of Excellence FAME of the European Union sixth framework program.

References

[1] F. Rodríguez-Reinoso, in: J.W. Patrick (Ed.), Porosity in Carbons, Wiley, Chichester, UK, 1995, p. 253.
[2] M. Che, O. Clause, C. Marcilly, in: G. Ertl, H. Knözinger, J. Weitkamp (Eds.), Handbook of Heterogeneous Catalysis, Wiley–VCH, Weinheim, 1997, p. 191.
[3] R. Schlögl, in: G. Ertl, H. Knözinger, J. Weitkamp (Eds.), Handbook of Heterogeneous Catalysis, Wiley–VCH, Weinheim, 1997, p. 138.
[4] F. Rodríguez-Reinoso, Carbon 36 (1998) 159.
[5] C. Prado-Burguete, A. Linares-Solano, F. Rodríguez-Reinoso, C. Salinas-Martínez de Lecea, J. Catal. 115 (1989) 98.
[6] M.A. Fraga, E. Jordão, M.J. Mendes, M.M.A. Freitas, J.L. Faria, J.L. Figueiredo, J. Catal. 209 (2002) 355.
[7] G.M. Pajonk, A. Venkateswara Rao, N. Pinto, F. Ehrburger-Dolle, M. Bellido Gil, in: B. Delmon, P.A. Jacobs, R. Maggi, J.A. Martens, P. Grange, G. Poncelet (Eds.), Preparation of Catalysts VII, in: Stud. Surf. Sci. Catal., vol. 118, Elsevier, Amsterdam, 1998, p. 167.
[8] F.J. Maldonado-Hódar, M.A. Ferro-Garcia, J. Rivera-Utrilla, C. Moreno-Castilla, Carbon 37 (1999) 1199.
[9] F.J. Maldonado-Hódar, C. Moreno-Castilla, A.F. Pérez-Cadenas, Appl. Catal. B 54 (2004) 217.
[10] C. Moreno-Castilla, F.J. Maldonado-Hódar, Carbon 43 (2005) 455.
[11] M.N. Padilla-Serrano, F.J. Maldonado-Hódar, C. Moreno-Castilla, Appl. Catal. B 61 (2005) 253.
[12] H.T. Gomes, P.V. Samant, P. Serp, P. Kalck, J.L. Figueiredo, J.L. Faria, Appl. Catal. B 54 (2004) 175.
[13] P.V. Samant, J.B. Fernandes, C.M. Rangel, J.L. Figueiredo, Catal. Today 102–103 (2005) 173.
[14] P.V. Samant, M.F.R. Pereira, J.L. Figueiredo, Catal. Today 102–103 (2005) 183.
[15] N. Job, R. Pirard, J. Marien, J.-P. Pirard, Carbon 42 (2004) 619.
[16] N. Job, A. Théry, R. Pirard, J. Marien, L. Kocon, J.-N. Rouzaud, F. Béguin, J.-P. Pirard, Carbon 43 (2005) 2481.
[17] N. Job, B. Heinrichs, F. Ferauche, F. Noville, J. Marien, J.-P. Pirard, Catal. Today 102–103 (2005) 234.
[18] N. Job, B. Heinrichs, S. Lambert, J.-F. Colomer, B. Vertruyen, J. Marien, J.-P. Pirard, AIChE J. (2006), in press.
[19] N. Job, F. Panariello, J. Marien, M. Crine, J.-P. Pirard, A. Léonard, J. Non-Cryst. Solids 352 (2006) 24.
[20] A. Léonard, N. Job, S. Blacher, J.-P. Pirard, M. Crine, W. Jomaa, Carbon 43 (2005) 1808.
[21] A.J. Lecloux, in: J.R. Anderson, M. Boudart (Eds.), Catalysis: Science and Technology, vol. 2, Springer, Berlin, 1981, p. 171.
[22] C. Alié, R. Pirard, A.J. Lecloux, J.-P. Pirard, J. Non-Cryst. Solids 246 (1999) 216.
[23] E.W. Washburn, Proc. Nat. Acad. Sci. 7 (1921) 115.
[24] F. Rodríguez-Reinoso, M. Molina-Sabio, Adv. Colloid Interface Sci. 76–77 (1998) 271.
[25] J.L. Figueiredo, M.F.R. Pereira, M.M.A. Freitas, J.J.M. Órfão, Carbon 37 (1999) 1379.
[26] J.R. Anderson, Structure of Metallic Catalysts, Academic Press, London, 1975.
[27] G. Bergeret, P. Gallezot, in: G. Ertl, H. Knözinger, J. Weitkamp (Eds.), Handbook of Heterogeneous Catalysis, Wiley–VCH, Weinheim, 1997, p. 439.
[28] R.J. Farrauto, C.H. Bartholomew, Fundamentals of Industrial Catalytic Processes, Blackie Academic & Professionals, Chapman & Hall, London, UK, 1997, p. 436.
[29] A. E Aksoylu, M. Madalena, A. Freitas, J.L. Figueiredo, Appl. Catal. A 192 (2000) 29.
[30] A.E. Aksoylu, M. Madalena, A. Freitas, M.F.R. Pereira, J.L. Figueiredo, Carbon 39 (2001) 175.
[31] A.E. Aksoylu, J.L. Faria, M.F.R. Pereira, J.L. Figueiredo, P. Serp, J.-C. Hierso, R. Feurer, Y. Kihn, P. Kalck, Appl. Catal. A 243 (2003) 357.
[32] P.V. Samant, F. Gonçalves, M.M.A. Freitas, M.F.R. Pereira, J.L. Figueiredo, Carbon 42 (2004) 1321.
[33] C.N. Satterfield, Mass Transfer in Heterogeneous Catalysis, MIT Press, Cambridge, 1970.
[34] B. Heinrichs, J.-P. Schoebrechts, J.-P. Pirard, AIChE J. 47 (2001) 1866.
[35] C. Alié, F. Ferauche, A. Léonard, S. Lambert, N. Tcherkassova, B. Heinrichs, M. Crine, P. Marchot, E. Loukine, J.-P. Pirard, Chem. Eng. J. 117 (2006) 13.
[36] S.D. Lin, M.A. Vannice, J. Catal. 143 (1993) 539.
[37] C. Prado-Burguete, A. Linares-Solano, F. Rodríguez-Reinoso, C. Salinas-Martínez de Lecea, J. Catal. 128 (1991) 397.
[38] F. Rodríguez-Reinoso, I. Rodríguez-Ramos, C. Moreno-Castilla, A. Guerrero-Ruiz, J.D. López-González, J. Catal. 99 (1986) 171.